Myocardial bloodflow quantification using rubidium-82 PET

Sabine Koenders, PhD
September 30, 2022
Universiteit Twente, Enschede

Promotor:
Prof. C.H. Slump, PhD

Co-promotors:
J.A. van Dalen, PhD
J.D. van Dijk, PhD

Myocardial perfusion imaging (MPI) using positron emission tomography (PET) has a high diagnostic value in the detection of obstructive coronary artery disease (oCAD) and is growing in its use. The addition of myocardial blood flow (MBF) and myocardial flow reserve (MFR) measurements to the visual assessment of PET images is making its way into clinical routine. MBF and MFR provide valuable additional diagnostic and prognostic information about the extent and functional importance of possible stenosis to visual assessment of PET images.

To be able to quantify the MBF and MFR, a rest and pharmacological-induced stress scan are acquired and all data over time (dynamic) are needed. In the process of data acquisition, image reconstruction, post-processing and interpretation of quantitative myocardial PET, there are several pitfalls that can result in unreliable blood flow quantification. In order for MBF and MFR quantification to achieve its full clinical potential, the technical aspects of MBF and MFR quantification must be well understood and standardised so that reliable MBF and MFR values can be routinely produced.

The aim of this thesis was to study and optimise technical aspects to obtain reliable MBF and MFR values with rubidium-82 (Rb-82) PET MPI. Furthermore, we studied the clinical value of MFR in clinical practice.

First, we comment on a study conducted by Hoff et al. In our opinion their study, which compared the effect of different administered activities (1110 MBq versus either 740 MBq or 370 MBq) on relative MPI images and on MBF and MFR values, has extended the current knowledge on the (technical) pitfalls in MBF and MFR quantification using PET and contributes to the integration of flow quantification in clinical practice. There are different types of PET scanners available for MBF quantification with Rb-82 PET. Recent developments in PET technology include PET systems using silicon photomultipliers (SiPM)-based PET with digital readout instead of photomultiplier tubes (PMT)-based PET. We determined the value of SiPM-based PET MPI as compared to a PMT-based PET scanner. We showed that defect interpretation, interpreter's confidence and blood flow measurements were comparable between both systems. However, SiPM-based PET provided an improved image quality in comparison to PMT-based PET. Then, we determined the effect of different temporal sampling protocols on MBF and MFR quantification. A temporal sampling protocol is used to reconstruct the dynamic images which are used in a kinetic model for MBF and MFR quantification. We found that MFR seemed to be a more suitable parameter as MFR did not differ for any of the temporal sampling protocols as compared to a reference protocol. We determined the effect of correcting for a certain kind of patient motion, called myocardial creep, on MBF and MFR values. This so-called myocardial creep is presumably caused by an increasing depth of respiration and lung volume induced by regadenoson which causes the repositioning of the diaphragm and heart. We showed that myocardial creep is a frequent phenomenon as it was observed in 52% of our patients during the stress scan. We found that especially the MBF value in the right coronary artery territory was affected as the mean MBF decreased from 4.0 to 2.7 mL/min/g after correction for myocardial creep. Therefore, detection and correction of myocardial creep is necessary to provide reliable flow measurements. We therefore provided instructions on how to detect and correct for myocardial creep.

In clinical practice, visual assessment of Rb-82 PET MPI is usually combined with *global* MFR values to detect oCAD. However, small regional blood flow deficits then may remain unnoticed. We compared the diagnostic value of *regional* MFR to *global* MFR in the detection of

oCAD. We showed that regional MFR resulted in an improved detection of oCAD as compared to global MFR independent of the visual assessment. It is yet unclear how to combine visual assessment of Rb-82 PET data with quantitative myocardial flow values in situations where conclusions on the presence of oCAD are contradictory. Hence, we estimated the probability of oCAD for an individual patient as function of the MFR value in patients with a visually normal scan as well as in patients with a visually abnormal scan. We found that based on visual Rb-82 PET interpretation only, patients with >10% probability of oCAD can be distinguished from patients with <10% probability. However, there is a strong dependency of MFR on patient's individual probability of oCAD: these probabilities may range from <1% to >70% (see figure 1). Combining both visual interpretation and MFR results in a superior individual risk-assessment, which may impact treatment strategy. In clinical practice, cardiologists combine the imaging data, clinical data and type of symptoms to estimate a post-test likelihood and, if needed, determine a specific treatment strategy. Artificial intelligence can help to improve interpretation of all combined data and thereby diagnosis of patients with oCAD. Lastly, we aimed to develop and validate a machine learning (ML)-based model to diagnose oCAD. The ML model resulted in a similar diagnostic performance as compared to expert readers, as shown in figure 2, and may be deployed as a risk stratification tool. This study showed that utilisation of ML is promising in the diagnosis of oCAD.

s.s.koenders@isala.nl ♦
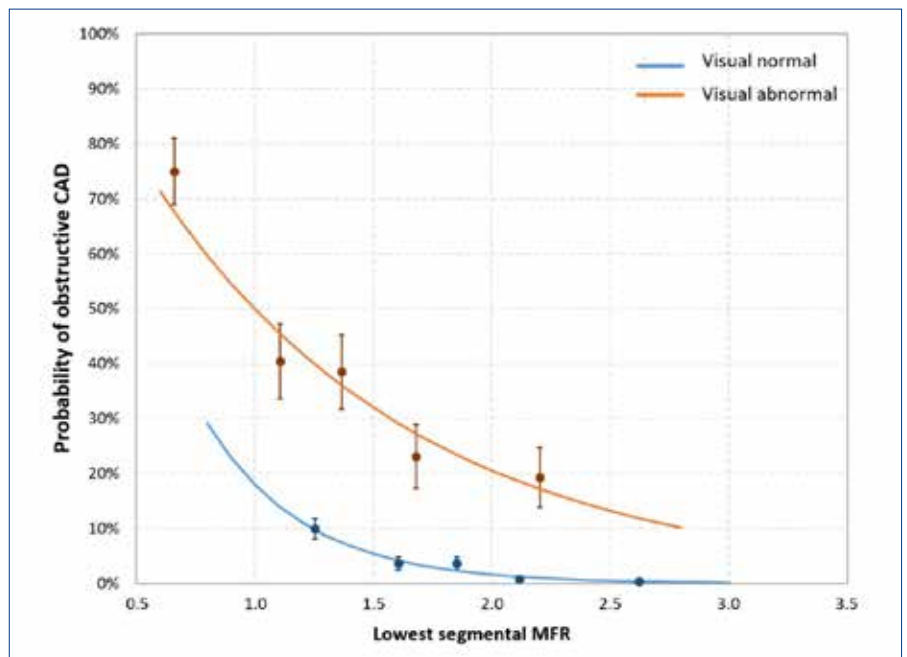
Figuur 3. Plot of the mean of each quintile (dot with error bars) and the lines showing the patient's probability (solid line) of having obstructive CAD for visually normal (blue) and abnormal (orange) scans combined with the lowest measured segmental MFR. The probability of obstructive CAD can be described for normal scans by $P_{oCAD} = 2.02 \cdot e^{-2.42 \cdot segMFR}$ ($R^2=0.94$) and for abnormal scans by $P_{oCAD} = 1.22 \cdot e^{-0.89 \cdot segMFR}$ ($R^2=0.94$).
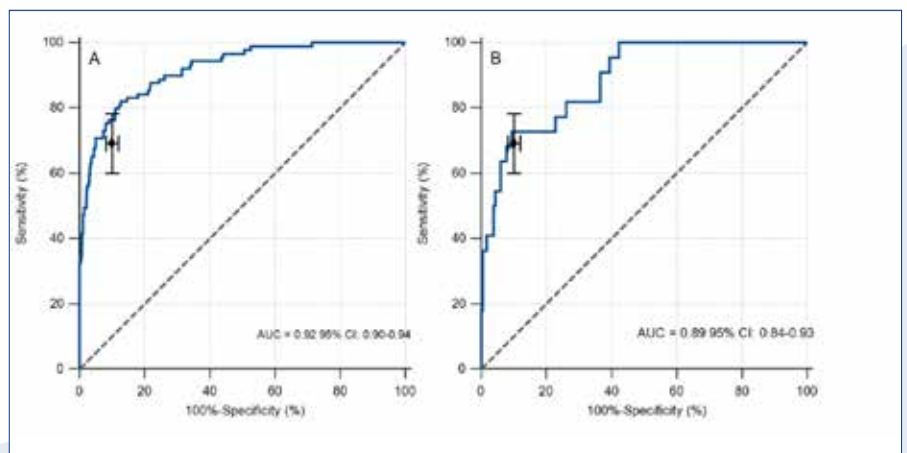
Figuur 2. ROC curve of the ML model for detection of obstructive CAD on the A) training (n=805) and B) test (n=202) dataset. The sensitivity and specificity of the expert readers, is plotted (black dot) with corresponding 95% confidence intervals.